

# Computational analysis of binding free energies between peptides and single-walled carbon nanotubes

Y. Cheng<sup>a,\*</sup>, G.R. Liu<sup>a,b</sup>, Z.R. Li<sup>a</sup>, C. Lu<sup>c</sup>

<sup>a</sup>Centre for ACES, Department of Mechanical Engineering, Singapore

<sup>b</sup>Singapore-MIT Alliance, National University of Singapore, 10 Kent Ridge Crescent, Singapore 119260, Singapore

<sup>c</sup>Inst. High Performance Comp. (IHPC), Singapore 117528, Singapore

Received 17 August 2005; received in revised form 14 November 2005

Available online 22 December 2005

## Abstract

Coating carbon nanotubes (CNTs) with peptides can solubilize the nanotubes in water solvent. To explore the utilization of CNTs in solvent and the affinities of CNTs for different peptides, binding free energies of peptides to single-walled carbon nanotubes (SWCNTs) are calculated and analyzed. The interactions between different peptides and SWCNTs are simulated using molecular dynamics (MD) methods. The binding free energies of peptides onto the outer-surface of the SWCNTs are then estimated based on thermodynamics theory. The estimated results of binding free energies are qualitatively comparable to binding affinities observed in experiments. Furthermore, the conformations of the binding peptides, as well as the energetic contributions to total binding free energies are analyzed to reveal the physical mechanisms of the interactions, which would be difficult to observe using experimental approaches. The van der Waals interaction is found to play a key role in binding of peptides to SWCNTs. Other effects such as hydrophobicity and aromatic rings of peptides are also examined. The findings of this study provide better understanding of the binding strength between proteins and CNTs, and therefore have potential applications in both scientific research and in industry for controlling CNT self-assembly, designing bio-functionalized CNTs as biosensors, and drug and gene delivery devices.

© 2005 Elsevier B.V. All rights reserved.

*Keywords:* SWCNTs; Peptides; Free energy; Binding; Molecular dynamics

## 1. Introduction

Since their discovery in 1991, carbon nanotubes (CNTs) have attracted great research interest due to their marvelous properties such as high electrical conductivity, excellent stiffness against bending, and high tensile strength. CNTs can have two distinct forms, single-walled carbon nanotubes (SWCNTs) and multi-walled carbon nanotubes (MWCNTs). Their unique mechanical and electrical properties facilitate the applications of CNTs in a large number of fields including biosensors [1] and atomic force microscopy [2,3]. Their applications in medicine and drug delivery are also promising [4].

\*Corresponding author. Tel.: +65 68744796; fax: +65 68744795.

E-mail addresses: [g0301103@nus.edu.sg](mailto:g0301103@nus.edu.sg) (Y. Cheng), [mpeliugr@nus.edu.sg](mailto:mpeliugr@nus.edu.sg) (G.R. Liu), [acelzr@nus.edu.sg](mailto:acelzr@nus.edu.sg) (Z.R. Li), [luchun@ihpc.a-star.edu.sg](mailto:luchun@ihpc.a-star.edu.sg) (C. Lu).

However, CNTs are highly hydrophobic and often form insoluble aggregates, due to which it is difficult to assemble CNTs into ordered or applicable structures. Bio-molecule functionalization is one option to overcome such defects. Many experimental efforts have been made, either through covalent or noncovalent interactions between bio-materials and CNTs. For example, by attaching functional groups covalently to nanotubes, CNTs have been made soluble in different solvent [5–9]. Their chemical and physical properties could be modified for various purposes of applications such as biosensors and drug delivery [10–12]. Noncovalent bond functionalization is another efficient approach. Some bio-materials could be encapsulated into the inner space of CNTs, or bound to the side-walls of CNTs [13–17].

In spite of these exciting observations through experimental methods, the mechanism of interactions between peptides and SWCNTs, remains unclear. Molecular simulation is a powerful tool which allows one to examine properties that are not accessible to experimental approaches. For example, it has been established through MD simulation that noncovalent interactions are major determinants in many physical interaction processes. A recent molecular dynamics (MD) simulation showed that SWCNTs could act as hydrophobic channels for conduction of water molecules [18]. It was also shown that DNA oligonucleotides could spontaneously insert into SWCNTs in water solvent environment [19]. Therefore, simulation work has been critical in exploring the physical properties of interactions between CNTs and biological materials.

In our previous work [20], we studied the self-insertion of peptides into SWCNTs, using MD simulations. Physical properties of the interaction were also explored. It was found that hydrophobicities of peptides had high positive correlations with their affinities for CNTs. Noncovalent interactions played a dominant role in their interaction processes. In this paper, binding of peptides to the outer-surface of SWCNTs is investigated. From a more intrinsic view, we analyze the binding free energies between peptides and SWCNTs, and investigate conformational characteristics involved in these processes.

Different methods have been developed to calculate the binding free energies between two biological molecules, based on the theory of thermodynamics [21]. For example, Massova and Kollman [22] developed an approach to estimate protein–protein interactions, and satisfactory agreement with experimental results was obtained. In this study, we use a method similar to that in Ref. [22], with modifications on energy modeling and data collection procedure so that the method will be well adapted to our problem.

In this work, the binding free energies between peptides and SWCNTs are estimated based on MD simulation results. Continuum water medium solvent is used to calculate energetic contributions. The binding free energy model used in this work takes into account the contributions of both the solute and the solvent. The change in free energies upon binding are compared with binding affinities reported from experiments. Furthermore, the energetic contributions are analyzed. Our results show that the five peptides tested have diverse affinities for CNTs. The van der Waals interaction is the most significant contributor. The interactions between aromatic rings have also been explored.

The findings of our study serve as a complement to experimental observations, which will provide clues on solubility of CNTs in water and techniques for controlling the interactions. It is clearly shown that the approach in this study benefits our understanding of the mechanism of the protein–CNT interaction, and hence facilitates the design of new nano-devices.

## 2. Methods

### 2.1. The generation of initial structures

To evaluate the free energies of peptides binding to SWCNTs, we adopt five peptide sequences. The experimental relative binding affinities of these peptides for CNTs are available [17]. Sequences of the peptides and their average hydrophobicities calculated by the K–D method [23] are listed in Table 1, for reference. A positive hydrophobicity value indicates that the peptide is hydrophobic, and the negative value corresponds to hydrophilic peptides. The higher the hydrophobicity values, the more hydrophobic the peptide is. Throughout the rest of the paper, we refer to the peptides by their assigned sequence numbers in Table 1, instead of listing the whole lengthy residue chains.

In order to estimate the free energy change upon binding, for each system we estimate, MD simulation experiment is carried out for the complex of the peptide and the SWCNT solvated in water, the peptide in

Table 1

Sequences of five 12-residue peptides simulated, as well as their average hydrophobicity. The hydrophobicity values of amino-acid residues are calculated using the K–D method.

Sequence number	Peptide sequence	Average hydrophobicity
1	HWKHPWGAWDTL	−1.067
2	HWKHPSGAWDTL	−1.058
3	HWSAWWIRSNQS	−1.083
4	HWSAWSIRSNQS	−1.075
5	LPPSNASVADYS	−0.192

water, and the SWCNT in water. The Amber99 force field, which has been shown to be suitable for general biological systems, is used for building amino-acid residues [24].

Initial structure of a SWCNT was constructed as a hollow cylinder rolled up from a graphite sheet. A (6, 6) type SWCNT with diameter of 8.1 Å and length of 25.8 Å is used. Carbon atoms on SWCNTs are uncharged particles with the van der Waals parameters of a cross-section  $\sigma_{cc} = 3.400$  Å and a potential well depth of  $\epsilon_{cc} = 0.086$  kcal/mol. Carbon–carbon bond lengths of 1.4 Å and bond angles of 120° are maintained by harmonic potentials with spring constants of 938 kcal/mol Å<sup>2</sup> and 126 kcal/mol rad<sup>2</sup>, corresponding to sp<sup>2</sup> carbon parameters in the AMBER99. For different types of atoms, the van der Waals interaction parameters are calculated using combination rules [25].

Initially, the peptide is constructed as a fully extended structure. Each complex of peptide–SWCNT contains one SWCNT and one peptide. The peptide is positioned approximately parallel to the SWCNT, and parts of them contact directly. Subsequently, the complex of peptide–SWCNT is surrounded by a layer of at least 10 Å of TIP3P water molecules [26]. Water molecules are not accessible to the contact regions of peptide–SWCNT complex. Periodic boundary conditions are applied throughout the simulation. In this model, all the particles (in this case, atoms) are enclosed in one box, which is duplicated in all the three dimensions to form one periodic array. The particles interact not only with other particles in one box, but also with all of their own images in neighboring boxes. The particles re-enter the box from the opposite box once they leave the box from one side. The total number of particles in the box is kept constant.

## 2.2. Molecular dynamics simulation in TIP3P water solvent

In this work, software package Amber7 is used to perform MD calculation [27]. The procedure of the MD simulation is described below. Firstly, for each initial structure of the complex, peptide or SWCNT solvated in explicit water molecules, energy minimization is performed to avoid steric clashes. The steepest descent method of minimization is used for the first 10 cycles and conjugate gradient minimization is run for the following 19,990 cycles. MD simulation of constant volume and constant temperature (NVT) ensemble is then run for 100 ps to raise the temperature from initial value of 0 K to 300 K. Subsequently the structure is simulated for 1 ns under the conditions of constant pressure and constant temperature (NPT) ensembles [28]. A time step of 1 fs is used to integrate Newton's equation of motion and the coordinates of the structures are saved every 5 ps. This simulation protocol helps to ensure the stability of the simulation process. Nonbonded cut-off of 8 Å is applied to truncate the long-range interaction to speed up the computation. The particle-mesh Ewald method (PME) algorithm with cubic-spline interpolation (1 Å grid width) is applied to calculate electrostatic interactions efficiently [29]. Bonds involving hydrogen atoms are constrained using the SHAKE algorithm [30].

## 2.3. Calculations of energy contributions

To calculate the free energies of peptide–SWCNT binding and the energy contributions, the Generalized Born Surface Area (GBSA) method is used [31]. The model implicitly represents water as continuum, which can efficiently calculate the electrostatic interaction of molecules in solvent. The final PDB structures of peptide–SWCNT complex, the SWCNT, and unbound peptides structures obtained from explicit solvent MD

simulation are then adopted for energy calculation in continuum models. After the removal of water molecules, 50 ps of MD simulations are carried out to arrive at the equilibrium state and another 50 ps for data collections. All the energy components are sampled by averaging the results over the final 50 ps.

As shown in Eq. (1), the binding free energy between a peptide and a SWCNT is estimated as the difference between the free energies of the complex in water solvent ( $G_{\text{complex}}^{\text{solvate}}$ ), and that of the sum of the SWCNT ( $G_{\text{nanotube}}^{\text{solvate}}$ ), the peptide ( $G_{\text{peptide}}^{\text{solvate}}$ ) solvated in water, respectively,

$$\Delta G = G_{\text{complex}}^{\text{solvate}} - (G_{\text{nanotube}}^{\text{solvate}} + G_{\text{peptide}}^{\text{solvate}}). \quad (1)$$

For each system, the value of the free energy is determined by its energy in vacuum, and the solvation free energy

$$G = E_{\text{vac}} + G_{\text{solvation}}, \quad (2)$$

where  $E_{\text{vac}}$  stands for the molecular mechanics energy of the solute in vacuum,  $G_{\text{solvation}}$  represents the contribution of the solvation-induced free energy. According to molecular mechanics theory,  $E_{\text{vac}}$  could be calculated as

$$E_{\text{vac}} = E_{\text{internal}} + E_{\text{vdw}} + E_{\text{ele}}, \quad (3)$$

which means that  $E_{\text{vac}}$  is composed of the internal energy ( $E_{\text{internal}}$ ), the van der Waals interaction energy ( $E_{\text{vdw}}$ ), and the electrostatic energy ( $E_{\text{ele}}$ ).

The internal energy includes the bond stretching, the angle bending and the torsion energy, which can be further expressed as

$$E_{\text{internal}} = E_{\text{bond}} + E_{\text{angle}} + E_{\text{torsion}}. \quad (4)$$

The contribution of the solvation free energy,  $G_{\text{sol}}$ , includes both the polar and nonpolar terms:

$$G_{\text{sol}} = G_{\text{pol}} + G_{\text{nonpol}}. \quad (5)$$

The polar ( $G_{\text{pol}}$ ) and nonpolar ( $G_{\text{nonpol}}$ ) energy contribution to the solvation free energy are estimated using GBSA. The polar term is calculated using

$$G_{\text{pol}} = \sum_{ij}^{\text{atoms}} \frac{q_i q_j}{f^{gb}(R_{ij})}. \quad (6)$$

The function  $f^{gb}$  estimates the reaction field potential [33]. Contributions of the nonpolar term are calculated proportional to the solvent accessible surface ( $A$ ) using Eq. (7). The surface area of the solute is computed using the model of LCPO [32], and  $\sigma = 0.005 \text{ kcal/mol } \text{\AA}^2$  [34].

$$G_{\text{nonpol}} = \sigma A. \quad (7)$$

Note that the energies and free energy contributions are all state functions. Therefore, we can calculate them at different stages of the interaction systems regardless of their paths of evolutions to these states.

In order to obtain a clear picture of the energy contributions, each term of  $\Delta E$  and  $\Delta G$  will also be listed, calculated as the difference of this value between two states before and after binding

$$\Delta E = E(\text{complex}) - (E(\text{peptide}) + E(\text{nanotube})). \quad (8)$$

The binding free energy can be finally calculated using

$$\Delta G = \Delta E_{\text{vac}} + \Delta G_{\text{solvation}} = \Delta E_{\text{internal}} + \Delta E_{\text{vdw}} + \Delta E_{\text{ele}} + \Delta G_{\text{pol}} + \Delta G_{\text{nonpol}}. \quad (9)$$

### 3. Results

#### 3.1. Peptides display diverse propensities

In the five peptide–SWCNT complex systems, the conformations of peptides change to favor interactions with SWCNTs. Some peptides wrap around the nanotubes completely while others partly contact the surface

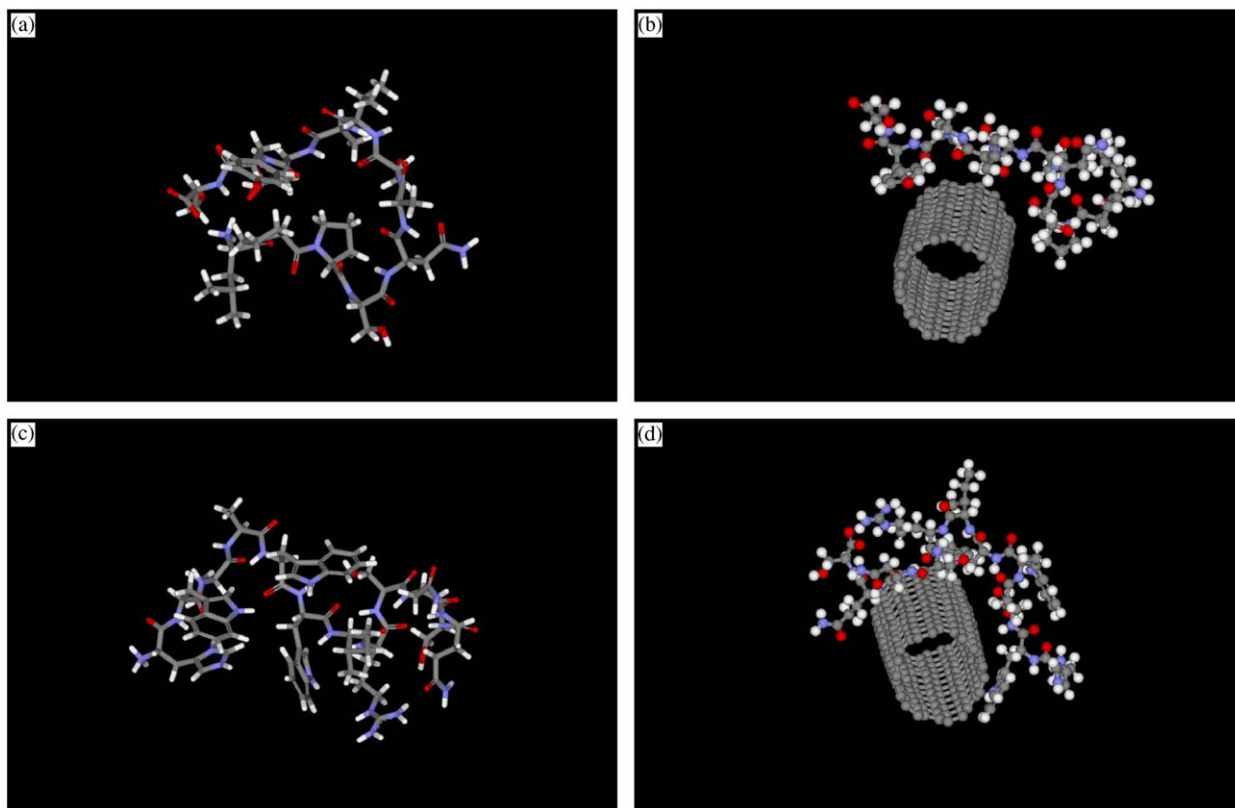


Fig. 1. Snapshots of final structures of peptides and peptide-SWCNTs in water solvent. (a) peptide 5, (b) peptide 5-SWCNT complex, (c) peptide 3, (d) peptide 3-SWCNT complex. The images were created with DS ViewerPro 5.0 software (Accelrys Inc., San Diego, CA).

of nanotubes. As observed from Fig. 1, peptide 5 (Fig. 1(a)) does not wrap the SWCNT completely, but it interacts more with water instead. Peptide 3 (Fig. 1(c)) binds tightly onto the SWCNT surface, which means that a larger part of the peptide interacts with the SWCNT. Apparently, the contact area of peptide 5 with the SWCNT surface is much smaller than that of peptide 3. Behaviors of unbound peptides solvated in water are also simulated and analyzed. Peptide 5 is folded, driven by the clustering in its end-groups. Peptide 3 shows a high tendency of clustering in aromatic rings. This structure implicates a favorable conformation of peptide 3 interacting with SWCNT, particularly for  $\pi$ - $\pi$  stacking of aromatic rings and SWCNT surfaces [17].

### 3.2. MD simulations of the systems in explicit solvent

To examine the convergences and stabilities of MD simulations, the energetic trajectories and structural changes are traced. The potential energy trajectories are analyzed with reference to simulation time. The mean value of the potential energies and their standard deviations during the last 500 ps are provided in supplemental information to verify the thermal stability of the simulations. The data demonstrates that the energies converge with small fluctuations.

The stability of the simulation is further studied through analysis of the root mean square deviations (RMSDs) of the backbone atoms on peptides, both in bound and unbound states. We provide one randomly selected RMSD trajectory of backbone atoms of peptide 3 in the two states in supplemental information. The RMSDs are stable with no unreasonable oscillations.

### 3.3. Free energy calculations and energetic analysis

Binding affinities between CNTs and peptides are sensitive to amino-acid sequences, implicating the design of nanotubes-based probes. To understand interactions between these two kinds of materials, analyzing the binding free energies between CNTs and different peptides sequence is an efficient and reliable approach.

For the five systems we calculated, the mean values of the absolute energy contributions and their standard deviations estimated from the 50 ps data-collection period are provided in Table 2. Overall, the energies remain constant and fluctuate within standard errors, except that  $E_{ele}$  and  $G_{pol}$  appear to have relatively large fluctuation. However, the energy sum of these two terms,  $E_{ele\_total}$  converges, and the errors are canceled by

Table 2

(a)–(e) The energy contributions of the five peptides binding to SWCNTs, and the standard deviations of the energy terms

Contributions (kcal/mol)	Peptide 1–SWCNT complex		Peptide 1		SWCNT	
	Mean	Std. dev.	Mean	Std. dev.	Mean	Std. dev.
$E_{internal}$	1638.3746	12.2537	276.6918	8.2177	1367.0123	9.0915
$E_{ele}$	−12.1162	60.7432	7.3884	66.93	0	0
$E_{edw}$	242.9762	7.5688	−23.9423	4.6645	309.2535	4.8121
$E_{vac}$	1869.2349	62.0499	260.1379	67.0886	1676.2667	8.3616
$G_{pol}$	−394.1432	60.7556	−425.8539	65.7464	0	0
$G_{nonpol}$	9.4334	0.2452	6.4378	0.284	3.8638	0.0123
$G_{sol}$	−384.7097	60.7575	−419.4159	65.6952	3.8638	0.0123
$E_{ele\_total}$	−406.2593	4.2575	−418.4655	4.4762	0	0
$G$	1484.525	11.2766	−159.2781	7.1467	1680.1296	8.3621

Contributions (kcal/mol)	Peptide 2–SWCNT complex		Peptide 2		SWCNT	
	Mean	Std. dev.	Mean	Std. dev.	Mean	Std. dev.
$E_{internal}$	1631.5192	12.0961	272.147	8.1537	1367.0123	9.0915
$E_{ele}$	142.6086	28.6066	170.8088	76.1325	0	0
$E_{edw}$	250.7564	4.3113	−25.6338	4.6942	309.2535	4.8121
$E_{vac}$	2024.8838	31.429	417.322	77.4235	1676.2667	8.3616
$G_{pol}$	−557.3611	28.412	−602.6929	75.0763	0	0
$G_{nonpol}$	9.9994	0.0369	5.7827	0.3024	3.8638	0.0123
$G_{sol}$	−547.3617	28.4117	−596.9105	74.9688	3.8638	0.0123
$E_{ele\_total}$	−414.7525	2.2455	−431.8842	4.6101	0	0
$G$	1477.5217	11.5573	−179.5883	7.5352	1680.1296	8.3621

Contributions (kcal/mol)	Peptide 3–SWCNT complex		Peptide 3		SWCNT	
	Mean	Std. dev.	Mean	Std. dev.	Mean	Std. dev.
$E_{internal}$	1638.374	12.8965	270.0867	10.5467	1367.0123	9.0915
$E_{ele}$	−345.1888	76.0889	−246.2108	91.7371	0	0
$E_{edw}$	244.1539	6.3216	−23.1936	5.4034	309.2535	4.8121
$E_{vac}$	1537.3383	75.3554	0.6823	91.2897	1676.2667	8.3616
$G_{pol}$	−319.562	74.7975	−417.1699	89.6081	0	0
$G_{nonpol}$	10.1645	0.1696	6.9329	0.3363	3.8638	0.0123
$G_{sol}$	−309.3974	74.8006	−410.2368	89.6046	3.8638	0.0123
$E_{ele\_total}$	−664.7509	5.5092	−663.3806	6.1703	0	0
$G$	1227.9415	11.772	−409.5546	7.8099	1680.1296	8.3621

Table 2 (continued)

(d)						
Contributions (kcal/mol)	Peptide 4–SWCNT complex		Peptide 4		SWCNT	
	Mean	Std. dev.	Mean	Std. dev.	Mean	Std. dev.
$E_{internal}$	1624.3468	13.0358	250.7221	8.4374	1367.0123	9.0915
$E_{ele}$	−409.3298	86.1343	−526.4892	96.0464	0	0
$E_{vdw}$	248.9652	6.7611	−28.4102	5.2523	309.2535	4.8121
$E_{vac}$	1463.9817	88.3124	−304.1774	96.097	1676.2667	8.3616
$G_{pol}$	−259.5987	85.1361	−144.1688	93.6886	0	0
$G_{nonpol}$	9.2655	0.1538	5.8317	0.2158	3.8638	0.0123
$G_{sol}$	−250.3332	85.1506	−138.3371	93.6964	3.8638	0.0123
$E_{ele\_total}$	−668.9283	5.2098	−670.658	5.8716	0	0
$G$	1213.6492	11.9748	−442.5143	7.44	1680.1296	8.3621

(e)						
Contributions (kcal/mol)	Peptide 5–SWCNT complex		Peptide 5		SWCNT	
	Mean	Std. dev.	Mean	Std. dev.	Mean	Std. dev.
$E_{internal}$	1582.9836	12.3242	219.3674	7.7071	1367.0123	9.0915
$E_{ele}$	−198.8516	64.7461	−293.2146	72.3533	0	0
$E_{vdw}$	267.3004	7.1236	−7.6251	4.8981	309.2535	4.8121
$E_{vac}$	1651.432	65.2193	−81.4723	72.9131	1676.2667	8.3616
$G_{pol}$	−268.2461	63.3083	−194.4066	71.0038	0	0
$G_{nonpol}$	9.0397	0.15	6.0703	0.1855	3.8638	0.0123
$G_{sol}$	−259.2063	63.2931	−188.3364	70.9858	3.8638	0.0123
$E_{ele\_total}$	−467.0977	4.1893	−487.621	4.0205	0	0
$G$	1392.226	10.6293	−269.8085	6.3475	1680.1296	8.3621

each other. Furthermore, one prolonged run for peptide 5 has been performed using the same method for 1 ns for testing, 500 ps for equilibrium and 500 ps for data collection. However, the longer period of simulation does not add to the convergence of the energy contributions.

Based on the results of MD simulations and the free energy calculations, the binding free energies  $\Delta G$  and energy contributions are shown in Table 3. In this table,  $\Delta G$  qualitatively correlates with the binding affinities between peptides and SWCNTs. The greater the free energy changes between the two states before and after binding, or the lower the value of  $\Delta G$ , the stronger the binding affinities. The peptide and the SWCNT should overcome certain value of energy barrier to dissociate once they bind to each other.

Fig. 2 lists the scaled experimental results of peptides' binding affinities to CNTs [17] and our calculated binding free energies. In the experimental study, values of plaque-forming units correlate with binding affinities. We qualitatively compare our estimated free energies with that of the plaque-forming units. Among the five peptides, absolute free-energy value of peptide 3 binding to CNT is the highest, corresponding to the strongest binding affinity observed in experiments. Furthermore, in agreement with experimental results, with only one mutation from Trp to Ser at the sixth position of peptide sequences—from peptide 1 to 2, and 3 to 4—both mutations show apparent influence on decreasing of the binding affinities.

The relative energy values are in good agreement with experiments, except for the calculation of peptide 5. Experimental results shows that peptide 5 has much weaker affinity for SWCNTs than peptides 1 and 3, but slightly stronger than peptides 2 and 4. In our simulation, binding free energy of peptide 5 to the SWCNT ranks the weakest among the five.

Although the calculated free energies qualitatively reflect experimental observations, the energy contributions and their roles in binding of peptides to SWCNTs remain unclear. We observe that the contributions of the internal energies are quite small, and hence nonbonded interactions play a dominant role.

Table 3  
The comparison of energy contributions of peptides binding to SWCNTs

Contributions (kcal/mol)	1	2	3	4	5
$\Delta E_{internal}$	-5.3295	-7.6401	1.275	6.6124	-3.3961
$\Delta E_{ele}$	-19.5046	-28.2002	-98.978	117.1594	94.363
$\Delta E_{vdw}$	-42.335	-32.8633	-41.906	-31.8781	-34.328
$\Delta E_{vac}$	-67.1697	-68.7049	-139.611	91.8924	56.6376
$\Delta G_{pol}$	31.7107	45.3318	97.6079	-115.43	-73.8395
$\Delta G_{nonpol}$	-0.8682	0.3529	-0.6322	-0.43	-0.8944
$\Delta G_{sol}$	30.8424	45.685	96.9756	-115.86	-74.7337
$\Delta E_{ele\_total}$	12.2062	17.1317	-1.3703	1.7297	20.5233
$\Delta G$	-36.3265	-23.0196	-42.6335	-23.9661	-18.0951

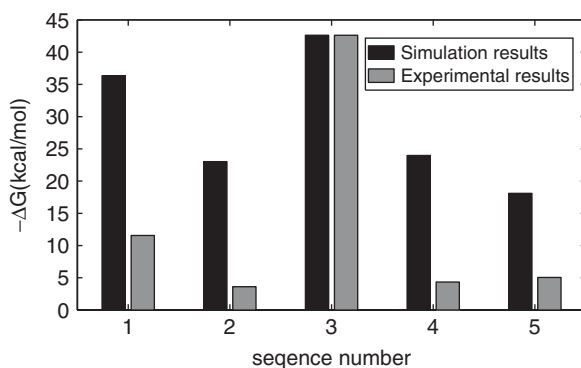


Fig. 2. The comparison of binding free energies with experimental results. The binding free energies are drawn as their absolute values (kcal/mol). The plaque-forming units from experimental results are scaled linearly in relation to the absolute values of the binding free energy of peptide 3. Larger  $\Delta G$  and plaque-forming unit values correspond to higher binding affinities.

It is also noted that the electrostatic interaction energy is balanced to some degree by the polar solvation energy. The sum of the two terms could be observed by  $E_{ele\_total}$ . The polar contribution of the solvation screens much of the electrostatic interaction in gas-phase, so that the value of  $\Delta E_{ele\_total}$  is much smaller than that of  $\Delta E_{ele}$  or  $\Delta G_{pol}$ . On the other hand, the contribution of the nonpolar solvation energy to the total binding energy is almost negligible. Therefore, it seems that the van der Waals interaction is the driving force for the binding process. For example, both peptides 1 and 3 have stronger van der Waals interactions, and they have stronger binding affinities. Table 4 shows the binding free energy differences between peptides 1 and 2, and peptides 3 and 4. There is only one mutation from Trp to Ser at the sixth position of the peptide sequences for both pairs. This results in an unfavorable loss of binding free energies. While comparing interaction energies of peptide 1–SWCNT with that of peptide 2–SWCNT complex, there's a loss of 9.47 kcal/mol in the van der Waals interaction and 4.93 kcal/mol in  $\Delta E_{ele\_total}$ , the sum of  $\Delta E_{ele}$  and  $\Delta G_{pol}$ . The mutation from peptides 3 to 4 leads to a loss of 10.24 kcal/mol in the van der Waals interaction and 2.43 kcal/mol in  $\Delta E_{ele\_total}$ . In both cases, although  $\Delta E_{ele}$  and  $\Delta G_{pol}$  have different trends of fluctuation, their summation shows a slight loss after the mutation. There is a stronger contribution of the van der Waals interaction before the mutation from Trp to Ser. The major loss in binding free energy is due to the loss of this interaction.

### 3.4. The effect of aromatic rings

The interactions between aromatic rings appear to be essential for the binding of peptides to SWCNTs. It has been observed experimentally that aromatic rings affected ligands or peptides' affinities for CNTs significantly [16,17].

We also obtain similar results through calculations of the five peptides' affinities for SWCNTs. As discussed in the previous section, peptide 2 has only mutation from peptide 1 at the sixth position, from Trp to Ser, and

Table 4

Relative binding free energies between peptides 1 and 2, and peptides 3 and 4.  $\Delta\Delta G$  of peptides 1–2 is calculated as  $\Delta\Delta G = \Delta G(\text{peptide 1-SWCNT}) - \Delta G(\text{peptide 2-SWCNT})$ , and the same with other energy contributions and that of peptides 3–4

Contributions (kcal/mol)	Peptide 1–2	Peptide 3–4
$\Delta\Delta E_{\text{internal}}$	2.3106	−5.2929
$\Delta\Delta E_{\text{ele}}$	8.6956	−206.4158
$\Delta\Delta E_{\text{vdw}}$	−9.4717	−10.2413
$\Delta\Delta E_{\text{vac}}$	1.5352	−221.95
$\Delta\Delta G_{\text{pol}}$	−13.6211	203.9839
$\Delta\Delta G_{\text{nonpol}}$	−1.2211	−0.2019
$\Delta\Delta G_{\text{sol}}$	−14.8426	203.782
$\Delta\Delta E_{\text{ele\_total}}$	−4.9255	−2.4319
$\Delta\Delta G$	−13.3069	−18.168

the same mutation is from peptides 3 to 4. It is found that significant propensity-changes result from this crucial mutation. We also observe the snapshots of peptide 3–SWCNT complex conformation over the course of the MD simulation. The orientation of planar of aromatic ring on Trp of the sixth position of peptide 3 approximately parallels the CNT surface, with an offset from the rings in CNT surface. This is also called an “offset stacked” interaction configuration [35]. The configurational trace reveals that a stable structure is formed due to the aromatic affinities within the peptide–CNT complex. Aromatic rings on other positions of the peptide may interact with the CNT surface with edge-to-face or other contact configurations.

Based on the results that the van der Waals interaction dominates the binding of peptides to SWCNTs, we expect that the stacked structure leads to stronger interaction energy. In order to further clarify the interaction mechanisms between aromatic rings and SWCNTs, a complex comprised of only one residue of Trp and one SWCNT is simulated for energy calculation. The complex in explicit water solvent is simulated first to obtain the equilibrium structure. The final equilibrium structure shows that the aromatic ring on the residue Trp also presents offset stacked configuration towards rings on the SWCNT. Afterwards, the complex structure is adopted for potential energy calculation in vacuum. The Trp residue is located at different positions along the length of the SWCNT, each separated by approximately the length of the radius of one aromatic ring, with the trajectory parallel to the CNT axis. On the other hand, the residue is positioned in a greater distance from the CNT surface, which is approximately the radius of an aromatic ring. Potential energies of the system with Trp in these different positions are calculated repeatedly with restrained structures. Analysis of the results indicates that the potential energy fluctuation along the length of CNT surface is quite small. The energy difference is within the range of 1 kcal/mol. However, potential energy change depending on the distance between the ring and CNT surface is much more substantial, the energy increases by 8.3 kcal/mol as the distance is enlarged approximately the radius of a ring. Despite the variations of the potential energy at different locations on the CNT surface, the distance between aromatic rings on the amino-acid residue and the CNT surface is more crucial, at least within certain range. Therefore, the stacked conformation is expected to possess stronger van der Waals interaction, and therefore leads to an optimized lower free energy.

#### 4. Discussions and directions of future work

##### 4.1. Functionalizing SWCNTs with peptides

One of the main challenges in applications of CNTs is the dispersion of nanotubes in solution and control of their assembly in solvent. Coating the CNTs with peptides could enable peptides to interact noncovalently with CNTs and therefore is one approach to modify the solubility of SWCNTs. Average hydrophobicities of the five peptides investigated in this paper are all slightly below zero, which indicates that on the whole, these peptides are prone to be hydrophilic and are in favor of interacting with water. When hydrophilic peptides are used to coat the CNTs, the tubes will be more soluble in water, instead of being highly hydrophobic.

#### 4.2. The influence of average hydrophobicities and aromatic rings of peptides

Previous simulation studies showed, in case of self-insertion of peptides into SWCNTs, the average hydrophobicities of peptides were crucial in determining their affinities for SWCNTs [20]. Distribution of hydrophobicity through a peptide also influenced the peptide–SWCNT affinity [17]. However, it was observed that peptides with lower values of average hydrophobicities may show high affinities for SWCNTs, when they contain aromatic rings. On comparing the sequences of the five simulated peptides, their comparable average hydrophobicities are inferred. The distributions of hydrophobicity values of residues (hydrophobic in center region and hydrophilic at the ends) are also similar. However, these five peptides differentiate in their affinities for SWCNTs. For a peptide, hydrophobicity properties on its own can not determine its affinity for SWCNT. Aromatic rings also make contributions here, concluded both from energetic analysis and conformational observation. The stacked structure of aromatic rings may decrease the hydrophobic surface exposed to solvent. The van der Waals interaction is also stronger for such structure.

#### 4.3. The electrostatic properties of SWCNTs

In this study, carbon atoms on SWCNTs are modeled as uncharged atoms due to the difficulty on calculating charge distributions on nanotubes. Therefore, no electrostatic interaction is involved in peptide–SWCNT interaction. However, the introduction of the SWCNT influences the distribution of atoms in the system, leading to the change of internal electrostatic energy of the peptide as well as the polar solvent energy contribution between the two states (before and after binding). The van der Waals interaction plays an important role [36], but it may not be sensitive to electronic influence of this process. Therefore  $\pi$ – $\pi$  interactions may not be expressed accurately. With the consideration of charge distributions on SWCNTs, the significance of  $\pi$ – $\pi$  interactions is expected to be even greater.

#### 4.4. Calculations of the entropic term

Energy contributions are summed unweighted to calculate the change of free energies while other types of contributions are not considered, such as the entropic change of solute. The entropy calculation is one of the greatest challenges in MD simulation, and accurate and complete estimation for entropy through MD calculation is still under exploration. Some studies added the vibrational, transitional, and torsional terms of the entropy of the solute to the binding free energies [22], which were options for estimation of the entropy, but these approaches might not be complete and accurate.

In our study, the structure of SWCNT is stable, almost remains unchanged through energetic analysis and conformational observation, and the peptides in five systems are of the same length. Regarding the entropy, the possible phases accessible to the peptide should be quite similar to each other. We may expect the entropy terms to cancel each other when the relative binding free energies are compared. Similar findings are also observed in previous study [22].

Although qualitatively acceptable agreement with experimental results has been obtained, the model is subject to optimize, given that more quantity results are available to be referred by simulation approaches. For example, prefactors could be added to terms of  $\Delta E_{internal}$ ,  $\Delta E_{ele}$ ,  $\Delta E_{vdw}$ ,  $\Delta G_{pol}$ , and  $\Delta G_{nonpol}$  in Eq. (9) to obtain their weighted sum of  $\Delta G$ , which may implicitly include the entropic contribution [21].

### 5. Conclusions

In this study, free energies of peptides binding to SWCNTs are calculated based on combined simulation methods of MD and continuum solvation model. The binding free energies take into account both contributions of the solute and solvent. The calculation results of binding free energies are proven to be satisfactory, compared with experimental results of binding affinities of different peptides for SWCNTs.

The energy contributions are also analyzed, and it is found that noncovalent bond interactions dominate this binding process, among which the van der Waals interaction appears to be the most significant

contributor. Aromatic rings on peptides have strong affinities for CNT surface, which is also driven by the van der Waals interaction.

Despite the difficulties on estimation of some terms contributing to the total free energy, such as entropic change of the solute, the method we adopt in the paper is a good estimation of the binding affinities between peptides and CNTs. The method is also applicable for calculation of the interaction energies between other non-biological materials and biological materials.

## Appendix A. Supplemental information

The online version of this article contains additional supplementary data. Please visit [doi:10.1016/j.physa.2005.11.033](https://doi.org/10.1016/j.physa.2005.11.033).

## References

- [1] F. Balavoine, P. Schultz, C. Richard, V. Mallouh, T.W. Ebbesen, C. Mioskowski, Helical crystallization of proteins on carbon nanotubes: a first step towards the development of new biosensors, *Angew. Chem.* 38 (13/14) (1999) 1912–1915.
- [2] S.P. Jarvis, T. Uchihashi, T. Ishida, H. Tokumoto, Y. Nakayama, Local solvation shell measurement in water using a carbon nanotube probe, *J. Phys. Chem. B* 104 (26) (2000) 6091–6094.
- [3] J. Li, A.M. Cassell, H. Dai, The carbon nanotube as AFM tips: measuring DNA molecules at the liquid/solid interface, *Surf. Interface Anal.* 28 (1999) 8–11.
- [4] A.R. Harutyunyan, B.K. Pradhan, G.U. Sumanasekera, E.Yu. Korobko, A.A. Kuznetsov, Carbon nanotubes for medical applications, *Eur. Cells Mater.* 3 (Suppl. 2) (2002) 84–87.
- [5] W. Zhao, C. Song, P.E. Pehrsson, Water-soluble and optically pH-sensitive single-walled carbon nanotubes from surface modification, *J. Am. Chem. Soc.* 124 (2002) 12418–12419.
- [6] A. Hirsch, Functionalization of single-walled carbon nanotubes, *Angew. Chem. Int. Ed. Engl.* 41 (2002) 1853–1859.
- [7] V. Georagakilas, K. Kordatos, M. Prato, D.M. Guldi, M. Holzinger, A.J. Hirsch, A Organic functionalization of carbon carbon nanotubes, *J. Am. Chem. Soc.* 124 (2002) 760–761.
- [8] V. Georagakilas, N. Tagmatarchis, D. Pantarotto, A. Bianco, J.-P. Briand, M. Prato, Amino acid functionalisation of water soluble carbon nanotubes, *Chem. Commun.* 24 (2002) 3050–3051.
- [9] D. Pantarotto, C.D. Partidos, J. Hoebeke, F. Brown, E. Kramer, J.P. Briand, S. Muller, M. Prato, A. Bianco, *Chem. Biol.* 10 (10) (2003) 961.
- [10] C.V. Nguyen, L. Delzeit, A.M. Cassel, J. Li, J. Han, M. Meyyappan, Preparation of nucleic acid functionalized carbon nanotube arrays, *Nano Lett.* 2 (2002) 1079–1081.
- [11] K.A. Williams, P.T.M. Veenhuizen, B.G. de la Torre, R. Eritjia, C. Dekker, Carbon nanotubes with DNA recognition, *Nature* 420 (2002) 761.
- [12] D. Pantarotto, C.D. Partidos, R. Graff, J. Howbeke, J.-P. Briand, M. Prato, A. Bianco, Synthesis, structural characterization and immunological properties of carbon nanotubes functionalized with peptides, *J. Am. Chem. Soc.* 125 (2003) 6160–6164.
- [13] Y. Gogotsi, J.A. Libera, A. Guvenc-Yazicioglu, C.M. Megaridis, In-situ multiphase fluid experiments in hydrothermal carbon nanotubes, *Appl. Phys. Lett.* 79 (2001) 1021–1023.
- [14] K. Hirahara, K. Suenaga, S. Bandow, H. Kato, T. Okazaki, H. Shinohara, S. Iijima, One-dimensional metallofullerene crystal generated inside single-walled carbon nanotubes, *Phys. Rev. Lett.* 85 (2000) 5384.
- [15] B.W. Smith, M. Monthieux, D.E. Luzzi, Encapsulated C<sub>60</sub> in carbon nanotubes, *Nature* 396 (1998) 323.
- [16] R.J. Chen, Y.G. Zhan, D.W. Wang, H. Dai, Noncovalent sidewall functionalization of single-walled carbon nanotubes for protein immobilization, *J. Am. Chem. Soc.* 123 (2001) 3838–3839.
- [17] S. Wang, E.S. Humphreys, S.Y. Chung, D.F. Delduco, S.R. Lustig, H. Wang, K.N. Parker, N.W. Rizzo, S. Subramoney, Y.M. Chiang, A. Jagota, Peptides with selective affinity for carbon nanotubes, *Nat. Mater.* 2 (3) (2003) 196–200.
- [18] G. Hummer, J.C. Rasalah, J.P. Noworyta, Water conduction through the hydrophobic channel of a carbon nanotubes, *Nature* 414 (2001) 188–190.
- [19] H. Gao, Y. Kong, D. Cui, C.S. Ozkan, Spontaneous insertion of DNA Oligonucleotides into carbon nanotubes, *Nano Lett.* 3 (2003) 471–473.
- [20] G.R. Liu, Y. Cheng, M. Dong, Z.R. Li, A study on self-insertion of peptides into single-walled carbon nanotubes based on molecular dynamics simulation, *Int. J. Mod. Phys. C* 16 (8) (2005) 1239–1250.
- [21] V. Zoete, O. Michielin, M. Karplus, Protein–ligand binding free energy estimation using molecular mechanics and continuum electrostatics. Application to HIV-1 protease inhibitors, *J. Comput. Aided Mol. Des.* 17 (2003) 861–880.
- [22] I. Massova, P.A. Kollman, Computational alanine scanning to probe protein–protein interactions: a novel approach to evaluate binding free energies, *J. Am. Chem. Soc.* 121 (1999) 8133–8142.
- [23] J. Kyte, R.F. Doolittle, A simple method for displaying the hydrophobic character of a protein, *J. Mol. Biol.* 157 (1982) 105–132.

- [24] J. Wang, P. Cieplak, P.A. Kollman, How well does a restrained electrostatic potential (resp) model perform in calculating conformational energies of organic and biological molecules, *J. Comput. Chem.* 21 (2000) 1049–1074.
- [25] W.D. Cornell, P. Cieplak, C.I. Bayly, I.R. Gould, K.M. Merz Jr., D.M. Ferguson, D.C. Ferguson, D.C. Spellmeyer, T. Fox, J.W. Caldwell, P.A. Kollman, A second generation force field for the simulation of proteins, nucleic acids, and organic molecules, *J. Am. Chem. Soc.* 117 (1995) 5179–5197.
- [26] W.J. Jorgensen, J. Chandreskhar, J. Madura, R. Imprey, M. Klein, Comparison of simple potential functions for simulating water, *J. Chem. Phys.* 79 (1983) 926–935.
- [27] D.A. Case, D.A. Pearlman, J.W. Caldwell, T.E. Cheatham III, J. Wang, W.S. Ross, C.L. Slimmerling, T.A. Darden, K.M. Merz, R.V. Stanton, A.L. Cheng, J.J. Vincent, M. Crowley, V. Tsui, H. Gohlke, R.J. Rader, Y. Duan, J. Pitera, I. Massova, G.L. Seibel, U.C. Singh, P.K. Weiner, P.A. Kollman, Assisted Model Building with Energy Refinement 7 (AMBER 7), University of California, San Francisco, CA, 2002.
- [28] H.J.C. Berendsen, J.P.M. Postma, W.F. van Gunsteren, A.D. Nola, J.R. Haak, Molecular dynamics with coupling to an external bath, *J. Chem. Phys.* 81 (1984) 3684–3690.
- [29] T. Darden, D. York, L. Pedersen, Particle mesh Ewald: an  $N_{\log}(N)$  method for Ewald sums in large systems, *J. Chem. Phys.* 98 (1993) 10089–10092.
- [30] J.P. Rychaert, G. Ciccotti, H.J.C. Berendsen, Numerical integration of the Cartesian equations of motion of a system with constraints; molecular dynamics of *n*-alkanes, *J. Comput. Phys.* 23 (1977) 327–341.
- [31] V. Tsui, D.A. Case, Theory and applications of the generalized Born solvation model in macromolecular simulation. *Biopolymers, Nucleic Acid. Sci.* 56 (2001) 275–291.
- [32] J. Weiser, P.S. Shenkin, W.C. Still, Approximate atomic surfaces from linear combinations of pairwise overlaps (LCPO), *J. Comput. Chem.* 20 (1999) 217–230.
- [33] A. Onufriev, D. Bashford, D.A. Case, Modification of the generalized born model suitable for macromolecules, *J. Phys. Chem. B* 104 (2000) 3712–3720.
- [34] D. Sitkoff, K.A. Sharp, B. Honig, Accurate calculation of hydration free energies using macroscopic solvent models, *J. Phys. Chem.* 98 (1994) 1978–1988.
- [35] M.L. Waters, Aromatic interactions in model systems, *Curr. Opin. Chem. Biol.* 6 (2002) 736–741.
- [36] C.A. Hunter, J.K.M. Sanders, The nature of  $\pi$ - $\pi$  interactions, *J. Am. Chem. Soc.* 112 (1990) 5525–5534.